Title
Epithelial membrane protein-2 (EMP2) promotes angiogenesis in glioblastoma multiforme.

Journal
Journal of neuro-oncology, 134(1)

ISSN
0167-594X

Authors
Qin, Yu
Takahashi, Masamichi
Sheets, Kristopher
et al.

Publication Date
2017-08-01

DOI
10.1007/s11060-017-2507-8

Peer reviewed

HHS Public Access

Author manuscript

J Neurooncol. Author manuscript; available in PMC 2018 August 01.

Published in final edited form as:

J Neurooncol. 2017 August ; 134(1): 29–40. doi:10.1007/s11060-017-2507-8.

Epithelial Membrane Protein-2 (EMP2) Promotes Angiogenesis in Glioblastoma Multiforme

Yu Qin[1], **Masamichi Takahashi**[8], **Kristopher Sheets**[2], **Horacio Soto**[3], **Jessica Tsui**[4], **Panayiotis Pelargos**[3], **Joseph P. Antonios**[3], **Noriyuki Kasahara**[9], **Isaac Yang**[3,5,6], **Robert M. Prins**[3,6,7], **Jonathan Braun**[4,6], **Lynn K Gordon**[1,2], and **Madhuri Wadehra**[4,6]

[1]Department of Ophthalmology, Stein Eye Institute, University of California-Los Angeles, Los Angeles, CA 90095, USA.

[2]Department of Medicine, University of California-Los Angeles, Los Angeles, CA 90095, USA.

[3]Department of Neurosurgery, University of California-Los Angeles, Los Angeles, CA 90095, USA.

[4]Pathology and Laboratory Medicine, University of California-Los Angeles, Los Angeles, CA 90095, USA.

[5]Department of Radiation Oncology, University of California-Los Angeles, Los Angeles, CA 90095, USA.

[6]Jonsson Comprehensive Cancer Center, David Geffen School of Medicine, University of California-Los Angeles, Los Angeles, CA 90095, USA.

[7]Department of Molecular and Medical Pharmacology, David Geffen School of Medicine, University of California-Los Angeles, Los Angeles, CA 90095, USA.

[8]Department of Neurosurgery, National Cancer Center, Tokyo, Japan.

[9]Department of Cell Biology and Pathology, University of Miami, Miami, FL 33136, USA.

Abstract

Glioblastoma Multiforme (GBM) is the most aggressive malignant brain tumor and is associated with an extremely poor clinical prognosis. One pathologic hallmark of GBM is excessive vascularization with abnormal blood vessels. Extensive investigation of anti-angiogenic therapy as a treatment for recurrent GBM has been performed. Bevacizumab, a monoclonal anti-vascular endothelial growth factor A (VEGF-A), suggests a progression-free survival benefit but no overall survival benefit. Developing novel anti-angiogenic therapies are urgently needed in controlling GBM growth. In this study, we demonstrate tumor expression of epithelial membrane protein-2 (EMP2) promotes angiogenesis both *in vitro* and *in vivo* using cell lines from human GBM. Mechanistically, this pro-angiogenic effect of EMP2 is partially through upregulating tumor VEGF-A levels. A potential therapeutic effect of a systemic administration of anti-EMP2 IgG1 on intracranial xenografts was observed resulting in both significant reduction of tumor load and

Conflicts of interests:

M.W., L.K.G, and J.B. are inventors on the University of California patents related to the anti- EMP2 IgG1 antibody presented in this work. They are also founders of Paganini Biopharma. No other authors have competing interests.

decreased tumor vasculature. These results suggest the potential for anti-EMP2 IgG1 as a promising novel anti-angiogenic therapy for GBM. Further investigation is needed to fully understand the molecular mechanisms how EMP2 modulates GBM pathogenesis and progression and to further characterize anti-EMP2 therapy in GBM.

Keywords

GBM; EMP2; angiogenesis; immunotherapy

Introduction

Glioblastoma Multiforme (GBM) is the most common, aggressive malignant brain tumor, affecting 3.2 per 100,000 adults each year in the USA. GBMs often present in patients as *de novo* grade IV astrocytoma and less frequently present as a lower grade (I–III) tumor [1]. The etiology of GBM is poorly understood and the standard-of-care treatment involves maximal surgical resection followed by radiation and chemotherapy with temozolomide [2]. Despite the multimodality treatment, the clinical outcome of GBM patients is extremely poor with a median survival of 12 months and a 5-year survival of less than 10% [1]. Two features of GBM present significant treatment challenges: 1) GBM is highly invasive which makes complete surgical resection almost impossible; 2) GBM is highly vascularized with abnormal vessels that appear disorganized, are large in diameter with thick basement membrane, and have low levels of pericytes [3]. The endothelial cells from patients with GBM are distinct and carry the same somatic mutations suggesting tumor endothelial cells originate from GBM peritumor niche [4,5]. While all the factors regulating angiogenesis in GBM are not known, one growth factor implicated in promoting GBM malignancy is vascular endothelial growth factor A (VEGF-A) [6]. Bevacizumab, a monoclonal antibody targeting VEGF-A, is currently a first-line treatment for recurrent GBM and shows a progression free survival benefit. However, there is no clear overall survival benefit [7,8]. Thus, a better understanding of GBM vasculature as well as novel anti-angiogenic therapy in GBM is urgently needed.

Epithelial membrane protein-2 (EMP2) is a member of the growth arrest specific-3 (GAS-3) family of tetraspan proteins. Previously we reported that EMP2 is present in most human GBM biopsies and undetectable in normal human brain tissues [9]. Furthermore, high EMP2 levels are associated with poor survival rates implicating it as an important prognostic and diagnostic marker. Mechanistically, EMP2 promotes GBM invasive phenotype in part through activating integrin-FAK-Src signaling [9]. In this study, we further examine the effect of EMP2 expression levels on GBM pathogenesis as well as the therapeutic benefit of anti-EMP2 IgG1 therapy. We demonstrate that EMP2 levels promote GBM neoangiogenesis partially through increasing VEGF-A levels. We also show that anti-EMP2 IgG1 antibody therapy dramatically reduce intracranial GBM tumor load and vasculature formation in tumor tissues. These results strongly support the utilization of EMP2-targeting therapy as an alternative anti-angiogenic therapy for GBM patients.

Materials and Methods

Cell Lines and Reagents

Human GBM cell lines T98, U118 or U87MG (ATCC, Manassas, VA) were cultured in DMEM supplemented with 10% fetal bovine serum (Hyclone Cat#30071), 1% glutamine, 1% penicillin and streptomycin, and 1% sodium pyruvate in a humidified 5% CO_2 incubator at 37°C. EMP2 expression was stably overexpressed or reduced using methods previously described [9]. Briefly, EMP2 was stably overexpressed using a retroviral vector encoding EMP2 and green fluorescent protein (GFP) or EMP2-GFP fusion protein. EMP2 expression was reduced using a lentiviral vector or an EMP2-specific ribozyme (RIBO), and for these cell lines an appropriate plasmid or shRNA vector control (CTRL) was used [9]. To create intracranial tumors, U87MG/EMP2, U87MG/CTRL and U87MG/shRNA were stably infected with a lentiviral vector containing firefly luciferase reporter gene (Luc) by the UCLA CURE Vector Core Facility. Cells were used within 2 months after resuscitation of frozen aliquots and were authenticated by the supplier. Cells were passaged every 2–4 days. Human umbilical vein endothelial cells (HUVEC; ATCC) were cultured in VTEC media as per manufacturer's instructions (Lonza, Allendale, NJ) and were used within the first 10 cell passages.

Intracranial U87MG Tumor Implantation

All animal experiments were performed in accordance with the Guide for the Care and Use of Laboratory Animals by the National Institutes of Health. The protocol was approved by the Office of Animal Research Oversight at UCLA. All efforts were made to minimize animal suffering. To create intracranial tumors, U87MG/ EMP2/Luc (n=6 mice), U87MG/ CTRL/Luc (n=11 mice), or U87MG/shRNA/Luc cells (n=12 mice) were stereotactically implanted into the right frontal lobe of 6–8-week-old female BALB/c athymic nude mice (Jackson Laboratory, Bar Harbor, ME) under adequate anesthesia. Specifically, tumor cells (1×10^5 in 2 μl sterile PBS for each mouse) were injected 2.8mm deep into right frontal lobe using a 26-gauge Hamilton syringe, 1mm anterior and 1.5mm lateral relative to the intersection of the coronal and sagittal sutures on the skull. Animal health was monitored for the behavioral and neurological abnormalities as well as weight loss. Tumor burden was monitored by bioluminescence imaging using IVIS200 as previously described [9]. Images were captured from day 1 to day 21 and day 18 imaging post tumor implantation was analysed This experiment was performed with 6 animals per group. To ensure the reproducibility of the results between the control and knockdown groups, a second experiment with another six animals was performed. The results from the first and second experiments were combined with one animal excluded due to over-inhalation of isoflurane during imaging.

To determine the anti-EMP2 IgG1 therapeutic effect, the EMP2-overexpressing cell line U87MG/EMP2/Luc cells (1×10^5 cells per 2 μl sterile PBS for each mouse) were stereotactically implanted into the right frontal lobe of 6–8-week-old female athymic nude mice under adequate anesthesia as described above. We have previously described the creation of an anti-EMP2 IgG1 antibody[10]. To ensure consistency among experiments, anti-EMP2 IgG1 was prepared in bulk by Lake Pharma on a contractual basis according to their

standard practices. Each antibody preparation includes a certificate of analysis ensuring the size, purity, and affinity of the antibody.

From day 1, mice were intraperitoneally injected with either control vehicle (n=5 mice) or anti-EMP2 full-length IgG1 antibody (n=6 mice) twice a week for three weeks. This first three anti-EMP2 antibody treatments were administered as 10 mg/kg body weight of mouse and last three anti-EMP2 treatments were 20 mg/kg body weight of mouse. Bioluminescence images were captured on days 1, 7, 14 and 21 post tumors implantation to monitor tumor growth. A two-way analysis of variance was used to determine the difference between control and anti-EMP2 IgG1 antibody treatment groups within treatment time course. Significance was defined as *p<0.05, ** p<0.001, *** p<0.0001.

Affymetrix RNA Microarray

RNA was extracted from cells that were genetically altered to change EMP2 expression levels. U118/EMP2, U118/CTRL or U118/shRNA cell lines were extracted using the Qiagen RNA isolation kits as per manufacturer's instruction (Qiagen Inc, Valencia, CA). Affymetrix U133 plus 2.0 microarray (Affymetrix, Santa Clara, CA) was performed in duplicate by UCLA Clinical Microarray Core Facility. Briefly, each RNA sample quality was validated by measuring absorbance 260/280, and samples in the range of 1.8–2.1 of 260/280 ratio were used for cDNA. RNA was converted to cDNA, hybridized onto microarray chips, followed by stringent washing and subsequent labeling with probes for automated visualization. An average of duplicate samples was taken and the relative abundance of specific gene expression was determined among groups. A heat map was created with R software (www.r-project.org) to identify differences and pathway analysis was created with Ingenuity software (www.ingenuity.com) by the UCLA Clinical Microarray Core Facility.

Immunohistochemistry

After euthanization, mouse brains were harvested and fixed in 10% formalin for 72 hours. Coronal cross sections of brain tumors were cut along the implant sites to expose tumors, followed by paraffin embedding. Tumor tissues were stained for CD34 to visualize endothelial cells [11]. Briefly, for antigen retrieval, sections were incubated at 95°C for 20 min in 0.1 M citrate buffer, pH 6. CD34 was detected using rabbit anti-human CD34 (Abcam, cat#81289) at a dilution of 1:100 at 4 °C overnight followed by visualization using the Vector ABC kit (Vector Labs, Burlingame, CA). Tumor sections were also stained with Masson's trichrome in order to visualize the collagen fibers within tumor tissues as per manufacturer's instruction (Polysciences Inc., Warminster, PA).

Image Analysis of CD34 Staining

CD34 staining of tumor tissues was analyzed with Image J software with a custom macro script. Specifically, images of CD34 stained vascular endothelia were captured in RGB format under 40X magnification and a 1360×1024 resolution using an Olympus BX51 microscope with a DP72 camera (Olympus Inc., Japan). Images were analyzed using the Fiji distribution of NIH ImageJ [12,13]. The blue channel had the best contrast ratio and was used for all subsequent image analysis steps. Images were segmented by thresholding intensity values using Otsu's method [14]. Objects in the resulting binary mask were closed using two

passes of dilation followed by two erosions. Any remaining small objects and salt-and-pepper noise were removed using two erosions followed by two dilations. Masked objects were used to measure the area of the original blue channel information. The results were tabulated to compared the difference among groups.

HUVEC Migration

2.5×10^5 T98, U118, U87MG cells that were genetically modified to vary in EMP2 expression were cultured in 6-well plates for 48 hours. Conditioned media were collected at the end of incubation. To determine the biologic effects of cell-secreted angiogenic factors into the conditioned media, 1×10^4 HUVEC cells were plated in the top chamber inserts of 24-well transwell (Corning Costar, Tewksbury, MA) and conditioned media from the cells were added into the bottom wells and the co-culture was incubated at 37°C for 5 hours. The filters of inserts were fixed with 3.7% formaldehyde at room temperature for 10 minutes and followed by staining with 0.1% crystal violet in 20% methanol at room temperature for 10 min. The migrated HUVEC cells were visualized using bright field microscopy. Migratory cell numbers were averaged by counting four random fields per transwell under 40× magnification. The experiment was repeated at least three times.

To determine the effect of the anti-EMP2 IgG1 antibody on cell-secreted angiogenic factors, 2.5×10^5 U87MG wild type cells were cultured in 6-well plates in the presence of 50 μg/ml anti-EMP2 full-length IgG1 antibody (n=4) or a vehicle control (n=3) for 48 hours. Conditioned media were collected at the end of incubation. HUVEC migration assay was performed as described above.

HUVEC Tube Formation

Conditioned media were collected as noted above from panels of T98, U118, and U87MG cells with varied EMP2 expression levels. Cover slips were placed in 24-well plates and coated with freshly thawed cold Geltrex LDEV-free reduced growth factor basement membrane matrix (ThermoFisher, Waltham, MA) diluted with ice cold PBS (1:1, vol/vol). Geltrex-coated cover slips were solidified at 37°C for 30 minutes and excess liquid was removed. 1×10^5 HUVEC cells were mixed in 500 μl conditioned media and added onto Geltrex-coated cover slips. Cells were incubated at 37°C for 16 hours. To visualize HUVEC cells, 4 μg/ml calcein (ThermoFisher) was added into cells at 37°C for additional 30 min. Tube formation was evaluated under a fluorescent microscope (Olympus BX51) and the number of fully formed capillary tubes were counted on the entire cover slips. The experiment was performed in triplicate and repeated at least three times.

SDS-PAGE/Western Blots

Cells were lysed in Laemmle sample buffer (62.5 mM Tris-Cl, pH 6.8, 10% glycerol, 2% SDS, 0.01% bromphenol blue, 2% β-mercaptoethanol). For detection of EMP2, lysates were de-glycosylated as described previously [9]. Proteins were separated by SDS-PAGE and transferred to nitrocellulose membranes (Amersham Biosciences, Pittsburg, PA). Membranes were blocked with 5–10% low fat milk in TBS containing 0.1% Tween-20 and probed with polyclonal anti-EMP2 antibody 1:2000, anti-VEGF-A 1:200 (Santa Cruz Biotechnology, clone A-20, sc-152, Dallas, TX) and anti-β-actin 1:10,000 (Sigma, A2228,

St Louis, MO), anti-phospho-STAT3 1:1000 (Cell Signaling, #9145, Danvers, MA), anti-STAT3 1:3000 (Cell Signaling, #4904, Danvers, MA), followed by HRP-conjugated secondary antibodies (Southern Biotechnology Associates, Birmingham, AL). Protein bands were visualized by chemiluminescence (Amersham Biosciences, Pittsburg, PA) and band intensities were quantified using NIH Image J software. All experiments were performed at least three times.

VEGF-A ELISA

To determine the cell-secreted VEGF-A levels, 2.5×10^5 T98, U118 or U87MG cells with varying EMP2 expressions were cultured in 6-well plates for 48 hours. Conditioned media were collected at the end of incubation. Secreted VEGF-A levels in conditioned media were examined with human VEGF Quantikine ELISA kit (DVE00, R&D Systems Inc., Minneapolis, MN) as per manufacturer's instruction. Briefly, conditioned media were added into 96-well anti-VEGF antibody coated-plates at room temperature for 2 hours. Following stringent washing three times, the samples were incubated with conjugated-VEGF antibody at room temperature for 2 hours. Following washing three times, substrates were added and VEGF-A levels were quantified in comparison with a standard curve using a SpectraMax 190 microplate reader (Molecular Devices, Sunnyvale, CA). To determine the effect of the anti-EMP2 IgG1 antibody on cell-secreted VEGF-A levels, 2.5×10^5 U87MG wild type cells were cultured in 6-well plates in the presence of 50 μg/ml anti-EMP2 full-length IgG1 antibody (n=4) or a vehicle control (n=3) for 48 hours. Conditioned media were collected at the end of incubation. VEGF-A ELISA was performed as noted above. Experiments were performed in duplicate and repeated three times.

Statistical Analysis

All values in the text are represented as the mean ± standard error of the mean (SE). Differences between means were determined using a one-way, two-way analysis of variance or student's *t* test as indicated in the figure legends or text. Significance in all cases was defined as $*p<0.05$, $** p<0.001$, $*** p<0.0001$.

Results

EMP2 Promotes GBM Angiogenesis in Intracranial U87MG Tumors

We previously showed that EMP2 overexpression promoted a more invasive phenotype while tumors with reduced levels of EMP2 produced smaller, less invasive tumors [9]. To extend this work, the vasculature of intracranial tumors derived from U87MG cells expressing different levels of EMP2 was examined. EMP2 expression was validated by Western blots prior to intracranial tumor implantation and increased (6 folds) or reduced (10 folds) EMP2 levels compared with control cells were stable during the experiments (Fig 1A). Consistent with previous findings, on day 18 post tumor implantation, reduction of EMP2 by shRNA (U87MG/shRNA) significantly decreased intracranial U87MG tumor growth compared to control scrambled shRNA (U87MG/CTRL). However, overexpression of EMP2 (U87MG/EMP2) did not increase the tumor mass based on bioluminescence imaging (Fig 1B).

Histological examination of the tumors suggested differences in tumor-associated vasculature. In order to confirm these effects, brain tumor sections were stained with CD34, a marker of endothelial cells. The CD34 staining revealed a striking difference among groups with more and larger blood vessels formed in U87MG/EMP2 and fewer, smaller blood vessels in U87MG/shRNA compared with U87MG/CTRL intracranial tumors (Fig 1C, left). Automated quantification using NIH Image J with a custom macro script for CD34 staining confirmed that U87MG/EMP2 tumors had significantly higher levels of CD34 staining compared to U87MG/CTRL and U87MG/shRNA (Fig 1D). Concordantly, tumor sections were stained with Masson's trichrome to differentiate tumors from surrounding connective collagen tissues and the results confirmed more collegen tissues (in blue) in U87MG/EMP2 and less in U87MG/shRNA compared with U87MG/CTRL tumors (Fig 1C, right). These data collectively suggest that EMP2 plays an important role in promoting angiogenesis and regulating tumor vasculature in GBM tumors *in vivo*.

EMP2-regulated Angiogenic Factors Potentiate HUVEC Migration and Capillary Tube Formation *in Vitro*

To characterize the effects of EMP2 on angiogenesis in GBM cell lines, *in vitro* endothelial cell functional assays were performed using panels of T98, U118 and U87MG cells which expressed different levels of EMP2 and have been previously described [9]. Conditioned media from panels of T98, U118 and U87MG revealed a significant positive correlation between EMP2 levels and HUVEC cell migration using a Boyden-chamber transwell migration assay (Fig 2A). To confirm and extend these results, the ability of EMP2 to promote capillary tube formation *in vitro* was determined. In two of the three cell lines, T98 and U118, conditioned media from cells with higher EMP2 levels enhanced capillary tube formation compared with the ones from control cells. In contrast to the other cell lines, under normoxic conditions, U87MG cells effectively formed endothelial tubes independent of EMP2 expression (Fig 2B). These results suggested that EMP2 levels promote endothelial recruitment and in some cases can promote more efficient tube formation.

EMP2 Increases VEGF-A Expression and Secretion in GBM Cells

Several pathways have been implicated in the regulation of angiogenesis in GBM. The best characterized angiogenic factor is VEGF-A, which has been shown to be indispensable for organ development as well as for growth in a number of tumors [15]. Given the evidence that EMP2 regulates endothelial cell migration and the critical role of VEGF-A in GBM, its expression was characterized in tumor cells with different levels of EMP2. Expression of VEGF-A was quantitated from panels of T98, U118 and U87MG normalized to β-actin (Fig 2C) and cell-secreted VEGF-A levels were determined by ELISA (Fig 2D). In all three cell lines, reduction in EMP2 by either ribozyme or shRNA produced a concomitant reduction in VEGF-A. Increased EMP2 appeared to directly upregulate VEGF-A in T98 cells but this effect was not statistically significant in U118 or U87MG (Fig 2C and 2D). These results suggest that EMP2 expression is required for VEGF-A production but perhaps there is a threshold beyond EMP2 cannot augment its translation. This also suggests that the increase in endothelial cell migration by increased EMP2 may be independent of VEGF-A.

U118 Affymetrix RNA Microarray

A number of pathways have been shown to modulate neoangiogenesis in GBM [16,17]. In order to characterize the transcriptional changes induced by modulating EMP2 levels, transcriptome profiling was performed using the Affymetrix U133 plus 2.0 Microarray. U118 cells were selected as EMP2 levels regulated both endothelial cell migration and capillary tube formation in this cell line. RNA from U118/EMP2, U118/CTRL or U118/shRNA was analyzed for comparison among groups for differential gene expression. The Venn diagram detailed gene expression between groups (Fig 3A). Among which 129 genes were expressed more than 1.5 fold between groups and 71 genes showed a reciprocal regulation between the three cell lines (Sup 1). Heat map analysis of these 129 genes displayed the differential gene profiling hierarchy among the three groups (Fig 3B). In addition, we performed the pathway analysis using Ingenuity software and identified 217 pathways that were associated with high EMP2 gene levels (EMP2 vs. CTRL, Sup 2).

EMP2 Regulates STAT3 in Some GBM Cells

In order to focus on the role of EMP2 in neoangiogenesis, pathways linked to GBM neoangiogenesis were further validated. Signal transducer and activator of transcription 3 (STAT3) is a transcriptional factor that modulates a diverse set of cellular functions including neoangiogenesis. Moreover, STAT3 activity has recently been implicated in driving GBM pathogenesis [18]. In order to validate and extend the regulation of STAT3 by EMP2, lysates were prepared as above from three GBM cell lines. STAT3 activation was determined by measuring its phosphorylation at tyrosine 705 normalized by total STAT3. The results showed heterogeneity among GBM cell lines. In panels of T98 and U118 cells, overexpression of EMP2 increased activated STAT3 whereas reduction of EMP2 reduced its activation compared with control cells. However, in contrast to the other two cell lines, there was no effect of EMP2 on STAT3 activation observed in panel of U87MG cells (Fig 3C). These results suggest that neoangiogenic signaling can be regulated by multiple pathways and may reflect the heterogeneity between different GBM cell lines.

Anti-EMP2 Reduces Intracranial U87MG/EMP2 Tumor Load and Angiogenesis

Our group have previously developed and characterized a humanized monoclonal anti-EMP2 IgG1 and examined its therapeutic effect in multiple model systems [9,10]. To further determine the application of this monoclonal antibody treatment in GBM, we established intracranial murine models using the more aggressive U87MG/EMP2 tumors. Tumor growth was monitored by bioluminescence imaging on day 1, 7, 14 and 21 post tumor implantation. Systemic anti-EMP2 IgG1 antibody treatment was initiated from day 1 post implantation. At day 14 and 21 we observed a significant reduction of tumor load from anti-EMP2 IgG1-treated animals compared to control vehicle-treated animals (Fig 4A). At day 21, intracranial tumors were collected and the gross histology and vasculature was assessed. Hematoxylin and eosin staining showed similar micro-metastases on the margins of the tumor (Fig 4B, left top) but significant changes were obtained in the tumor-associated vasculature. CD34 staining revealed a robust reduction in angiogenesis in anti-EMP2 IgG1-treated animals compared to the vehicle control-treated ones (Fig 4B, left bottom). Automated quantification of CD34 staining showed a 68.1% reduction in CD34 staining area in anti-EMP2 IgG1-

treated mice compared with control vehicle-treated mice (Fig 4B, right). These results suggest that anti-EMP2 IgG1 may be a novel anti-angiogenic therapy for GBM in this model system.

To further elucidate the mechanism of the antibody, U87MG cells were treated with the anti-EMP2 IgG1 antibody or a vehicle control and conditioned media were collected. HUVEC migration assay demonstrated a significant reduction in HUVEC cell recruitment in the presence of anti-EMP2 antibody compared with vehicle control (Fig 5A). Concordantly, VEGF-A expression in tumor cells (Fig 5B) and cell-secreted VEGF-A levels in conditioned media (Fig 5C) were also significantly decreased by treatment of anti-EMP2 IgG1 antibody compared with vehicle control. Both *in vivo* and *in vitro* studies demonstrated a promising therapeutic effect of anti-EMP2 IgG1 antibody in these GBM models that resulted in smaller tumor sizes and fewer tumor vasculatures.

Discussion

Despite numerous efforts in the research of GBM pathogenesis and multimodality treatment, the prognosis of GBM patients is still very poor [1]. In this report we demonstrate that EMP2 may be a promising therapeutic target due to its high specificity in GBM tumors and its effect in regulating multiple downstream targets including neoangiogenesis. EMP2 is present in over 90% GBM patient samples from human brain tumor tissue microarray but is absent in normal brain, suggesting its utility as a therapeutic and/or diagnostic target for the disease [9]. GBM tumors exhibit two classical hallmarks. They are typically highly invasive into surrounding brain parenchyma as well as excessive vascularization with abnormal blood vessels which appear disorganized, large in diameter with thick basement membrane and low levels of pericytes. Concordantly, high EMP2 levels in GBM are associated with a more invasive phenotype, and an increase in EMP2 by genetic engineering dramatically increased tumor invasion [9]. In this report, we further demonstrate that engineered, high EMP2 levels are associated with both an increase in number as well as size of blood vessels in GBM tumors. The effect of altered EMP2 levels on endothelial cells can be recapitulated *in vitro* as cell lines with higher EMP2 levels recruit more endothelial cells and in some cell lines is sufficient to induce neovascularization. This regulatory effect is in part due to upregulation of VEGF-A levels.

Anti-angiogenic therapies are currently in use as second line therapies for GBM. The FDA granted accelerated approval to bevacizumab as a single agent for patients with progressive disease, although it results in a progression-free survival benefit, it does not alter overall survival for patients with GBM. Recurrence for these patients has been associated with poor tumor oxygenation with the resulting bevacizumab resistant glioblastomas showing increased c-Met, focal adhesion kinase, and STAT3 phosphorylation [19–21]. In contrast to the anti-angiogenics on the market, anti-EMP2 therapy alters the tumor cell. Our group has previously developed and characterized a humanized monoclonal IgG1 antibody targeting EMP2 [10], and we examined its therapeutic effect using intracranial U87MG/EMP2 tumor xenografts. We find the systemic treatments using anti-EMP2 antibody significantly reduced tumor load by bioluminescence imaging and formed less vasculature in tumor tissues, suggesting it may be a promising novel anti-angiogenic therapy for GBM.

Using Affymetrix RNA microarray technology, modulation of EMP2 levels altered several signaling pathways. In this report, we focus on the pathways previously implicated in regulating neoangiogenesis. STAT3 activation regulates diverse cellular functions including neoangiogenesis. Persistent STAT3 phosphorylation is detectable in 70% of human tumors and in up to 83% of primary GBM [18]. JSI-124, a natural chemical compound and a potent STAT3 inhibitor, effectively inhibits VEGF-A expression, prevents HUVEC migration and capillary tube formation and also reduces invasiveness of GBM cells [22]. In our study, EMP2 increased STAT3 phosphorylation in T98 and U118 but not in U87MG panels, and we predict this discrepancy is likely due to the heterogeneity of molecular backgrounds of GBM cell lines. It is well established that GBM cell lines are highly heterogeneous, and this can include alterations in p53 and/or PTEN. Tumor suppressor p53 mutation is very common in GBM and seen in 25–30% of primary GBM and 60–70% of secondary GBM [23]. Phosphatase and tensin homolog (PTEN) mutations are observed in up to 40% of GBM tumors, and dual inactivation of p53 and PTEN in murine neural stem cells promotes undifferentiated tumors [24]. It is known, for example, that U87MG has a mutant PTEN but wild type p53 and is classified as an epithelial cell line. In contrast, U118 has both mutant PTEN and p53 and is characterized as mixed cell line, while T98 is typically characterized as a p53 mutant mesenchymal cell [25–27]. In this context, it has been shown that STAT3 can have varying effects based on PTEN status, where it can act as a tumor suppressor in some GBM cell lines with PTEN deficiency [28]. We thus predict that signaling from EMP2, a membrane protein, is upstream of these mutations, but its effect on STAT3 signaling can become more or less dominant depending on the other alterations within the cell. Likewise, the downregulation of EMP2 by the antibody inhibits tumor associated VEGF-A production with one direct effect being a decrease in VEGF secretion.

Drug delivery is one of the major formidable obstacles in treating GBM and standard systemically administered chemotherapy is often insufficient to deliver across intact blood brain barrier (BBB). The homeostasis of BBB is essential for normal brain functions. Detailed mechanisms of BBB are still elusive, but it is formed by the tight junctions of brain capillary endothelial cells surrounded by astrocytes, pericytes and microglial [29]. The intact BBB prevents passage of water-soluble compounds with a molecular weight greater than 180 Da; however, most chemotherapeutic agents have molecular weight greater than 200 Da [30]. In GBM, the BBB is compromised and leaky which leads to edematous swelling, increased intracerebral pressure, and possible passage of compounds with a greater molecular weight [29]. In this study, we predict that the anti-EMP2 IgG1 antibody may successfully cross the leaky BBB in a compromised state.

In conclusion, our study revealed a novel role for EMP2 in regulating GBM tumor-stromal interactions. EMP2 in the tumor promoted endothelial recruitment and vessel formation, and this effect could be recapitulated *in vivo*. We further show that anti-EMP2 IgG1 antibody therapy may be a novel anti-angiogenic treatment for GBM through a decrease in tumor-associated VEGF-A. Additional studies are needed to further translate the effects of the anti-EMP2 IgG1 to further explore how timing, dose, and other delivery methods (intratumor, intrathecal vs. systemic) may improve its utility.

Supplementary Material

Refer to Web version on PubMed Central for supplementary material.

Acknowledgments

We are thankful for the support and guidance of Dr. Emmanuelle Faure and Dr. Janet Treger of the UCLA/CURE Vector Core. This study was supported by NIH National Center for Advancing Translational Science (NCATS) UCLA CTSI Grant Number UL1TR001881, NCI R01 CA163971 (M.W.), a gift of Richard and Barbara Braun (J.B.), and the Oppenheimer Family Foundation (L.K.G).

Isaac Yang was partially supported by a Visionary Fund Grant, an Eli and Edythe Broad Center of Regenerative Medicine and Stem Cell Research UCLA Scholars in Translational Medicine Program Award, The Jason Dessel Memorial Seed Grant, the UCLA Honberger Endowment Brain Tumor Research Seed Grant, and the Stop Cancer (US) Research Career Development Award.

Panayiotis Pelargos was funded by the Gurtin SSCD and Skull Base Research Fellowship.

Abbreviations

GBM	glioblastoma multiforme
EMP2	epithelial membrane protein-2
VEGF-A	vascular endothelial growth factor A
STAT3	signal transducer and activator of transcription 3
PTEN	phosphatase and tensin homolog
BBB	blood brain barrier

References

1. Dolecek TA, Propp JM, Stroup NE, Kruchko C. CBTRUS statistical report: primary brain and central nervous system tumors diagnosed in the United States in 2005–2009. Neuro Oncol. 2012; 14(Suppl 5):v1–49. [PubMed: 23095881]
2. Omuro A, DeAngelis LM. Glioblastoma and other malignant gliomas: a clinical review. JAMA. 2013; 310:1842–1850. [PubMed: 24193082]
3. Liebelt BD, et al. Glioma Stem Cells: Signaling, Microenvironment, and Therapy. Stem Cells Int. 2016; 2016:7849890. [PubMed: 26880988]
4. Ricci-Vitiani L, et al. Tumour vascularization via endothelial differentiation of glioblastoma stem-like cells. Nature. 2010; 468:824–828. [PubMed: 21102434]
5. Wang R, et al. Glioblastoma stem-like cells give rise to tumour endothelium. Nature. 2010; 468:829–833. [PubMed: 21102433]
6. Lamszus K, et al. Levels of soluble vascular endothelial growth factor (VEGF) receptor 1 in astrocytic tumors and its relation to malignancy, vascularity, and VEGF-A. Clin Cancer Res. 2003; 9:1399–1405. [PubMed: 12684411]
7. Friedman HS, et al. Bevacizumab alone and in combination with irinotecan in recurrent glioblastoma. J Clin Oncol. 2009; 27:4733–4740. [PubMed: 19720927]
8. Kreisl TN, et al. Phase II trial of single-agent bevacizumab followed by bevacizumab plus irinotecan at tumor progression in recurrent glioblastoma. J Clin Oncol. 2009; 27:740–745. [PubMed: 19114704]
9. Qin Y, et al. Epithelial membrane protein-2 (EMP2) activates Src protein and is a novel therapeutic target for glioblastoma. The Journal of biological chemistry. 2014; 289:13974–13985. [PubMed: 24644285]

10. Fu M, et al. Rationale and preclinical efficacy of a novel anti-EMP2 antibody for the treatment of invasive breast cancer. Mol Cancer Ther. 2014; 13:902–915. [PubMed: 24448822]
11. Fina L, et al. Expression of the CD34 gene in vascular endothelial cells. Blood. 1990; 75:2417–2426. [PubMed: 1693532]
12. Schneider CA, Rasband WS, Eliceiri KW. NIH Image to ImageJ: 25 years of image analysis. Nat Methods. 2012; 9:671–675. [PubMed: 22930834]
13. Schindelin J, et al. Fiji: an open-source platform for biological-image analysis. Nat Methods. 2012; 9:676–682. [PubMed: 22743772]
14. Hetal J, Vala AB. A review on Otsu image segmentation algorithm. International Journal of Advanced Research in Computer Engineering & Technology (IJARCET). 2013; 2:387–389.
15. Hormigo A, Ding BS, Rafii S. A target for antiangiogenic therapy: vascular endothelium derived from glioblastoma. Proc Natl Acad Sci U S A. 2011; 108:4271–4272. [PubMed: 21383166]
16. Kaur B, Tan C, Brat DJ, Post DE, Van Meir EG. Genetic and hypoxic regulation of angiogenesis in gliomas. J Neurooncol. 2004; 70:229–243. [PubMed: 15674480]
17. Soda Y, Myskiw C, Rommel A, Verma IM. Mechanisms of neovascularization and resistance to anti-angiogenic therapies in glioblastoma multiforme. J Mol Med (Berl). 2013; 91:439–448. [PubMed: 23512266]
18. Luwor RB, Stylli SS, Kaye AH. The role of Stat3 in glioblastoma multiforme. J Clin Neurosci. 2013; 20:907–911. [PubMed: 23688441]
19. Jahangiri A, et al. Gene Expression Profile Identifies Tyrosine Kinase c-Met as a Targetable Mediator of Antiangiogenic Therapy Resistance. Clinical Cancer Research. 2013; 19:1773–1783. [PubMed: 23307858]
20. Das S, Marsden PA. Angiogenesis in Glioblastoma. New England Journal of Medicine. 2013; 369:1561–1563. [PubMed: 24131182]
21. Bonekamp D, et al. Assessment of tumor oxygenation and its impact on treatment response in bevacizumab-treated recurrent glioblastoma. Journal of Cerebral Blood Flow & Metabolism. 2016
22. Yuan G, et al. JSI-124 suppresses invasion and angiogenesis of glioblastoma cells in vitro. PLoS One. 2015; 10:e0118894. [PubMed: 25789853]
23. England B, Huang T, Karsy M. Current understanding of the role and targeting of tumor suppressor p53 in glioblastoma multiforme. Tumour Biol. 2013; 34:2063–2074. [PubMed: 23737287]
24. Zheng H, et al. p53 and Pten control neural and glioma stem/progenitor cell renewal and differentiation. Nature. 2008; 455:1129–1133. [PubMed: 18948956]
25. Djuzenova CS, et al. Actin cytoskeleton organization, cell surface modification and invasion rate of 5 glioblastoma cell lines differing in PTEN and p53 status. Exp Cell Res. 2015; 330:346–357. [PubMed: 25149900]
26. Diss E, et al. VorinostatSAHA Promotes Hyper-Radiosensitivity in Wild Type p53 Human Glioblastoma Cells. J Clin Oncol Res. 2014; 2
27. Patyka M, et al. Sensitivity to PRIMA-1MET is associated with decreased MGMT in human glioblastoma cells and glioblastoma stem cells irrespective of p53 status. Oncotarget. 2016
28. de la Iglesia N, et al. Identification of a PTEN-regulated STAT3 brain tumor suppressor pathway. Genes Dev. 2008; 22:449–462. [PubMed: 18258752]
29. Wolburg H, Noell S, Fallier-Becker P, Mack AF, Wolburg-Buchholz K. The disturbed blood-brain barrier in human glioblastoma. Mol Aspects Med. 2012; 33:579–589. [PubMed: 22387049]
30. Kroll RA, Neuwelt EA. Outwitting the blood-brain barrier for therapeutic purposes: osmotic opening and other means. Neurosurgery. 1998; 42:1083–1099. discussion 1099-1100. [PubMed: 9588554]

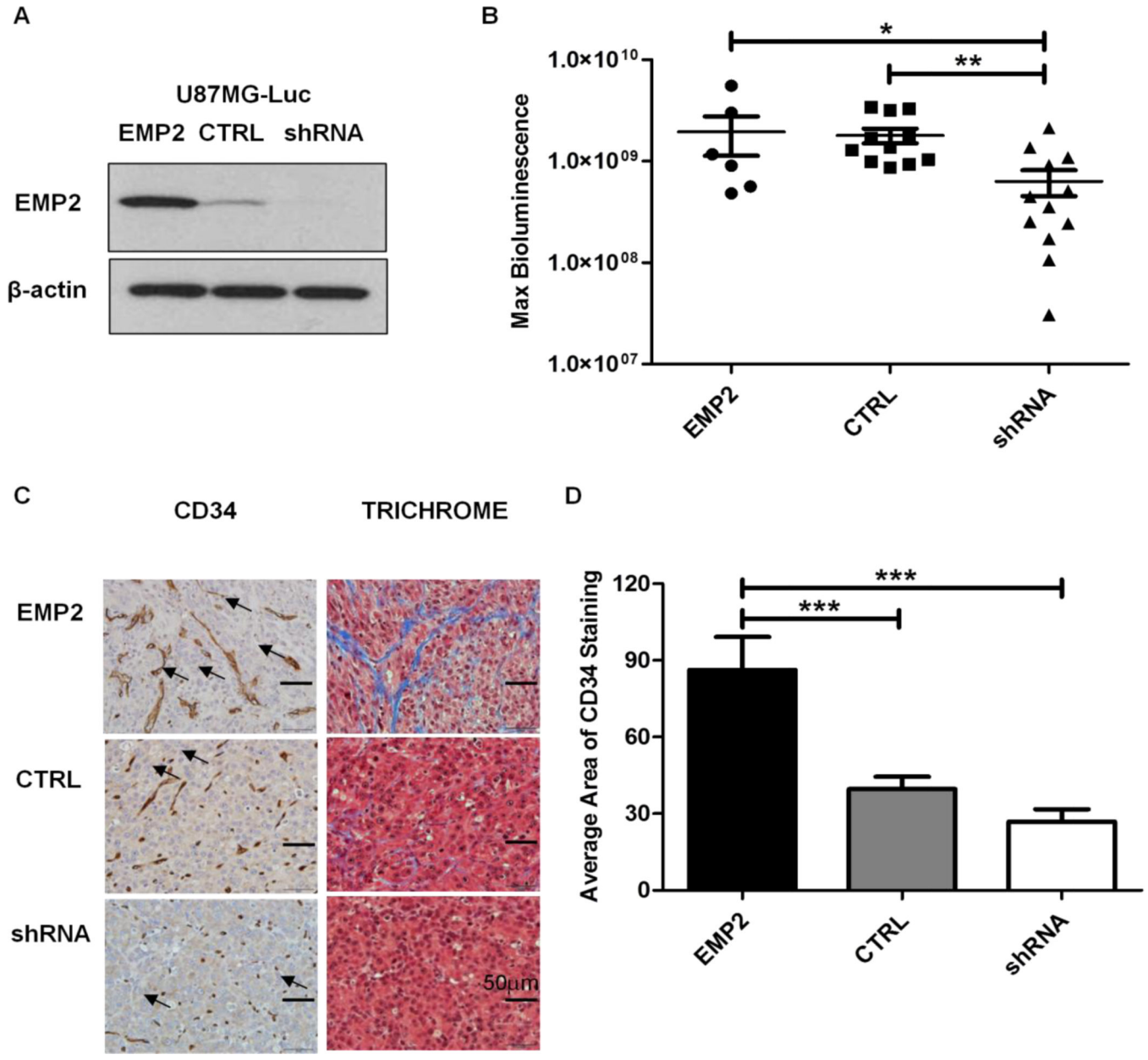

FIG 1. EMP2 Promotes Angiogenesis in U87MG Intracranial Tumors

(A) EMP2 levels were validated among the U87MG/Luc panel by Western Blots prior to stereotactic implantation. (B) Intracranial tumor growth was monitored by bioluminescence imaging on day 18 post tumor implantations in mice bearing U87MG/EMP2 (n=6), U87MG/CTRL (n=11) or U87MG/shRNA (n=12). The numbers of animals per group was generated by pooling two independent trials. (C) Intracranial tumors were fixed and stained with CD34 (left) and trichrome (right) and representative images were taken with a bright field microscope under 400× magnification. Arrowheads indicate representative staining of tumor associated vasculature. (D) Automated quantification of CD34 staining among groups was determined by NIH Image J software with a custom macro script as detailed in methods. One-way analysis of variance with a Bonferroni post-test was calculated to determine the

difference among three groups. Significance was defined as *$p<0.05$, ** $p<0.001$, *** $p<0.0001$.

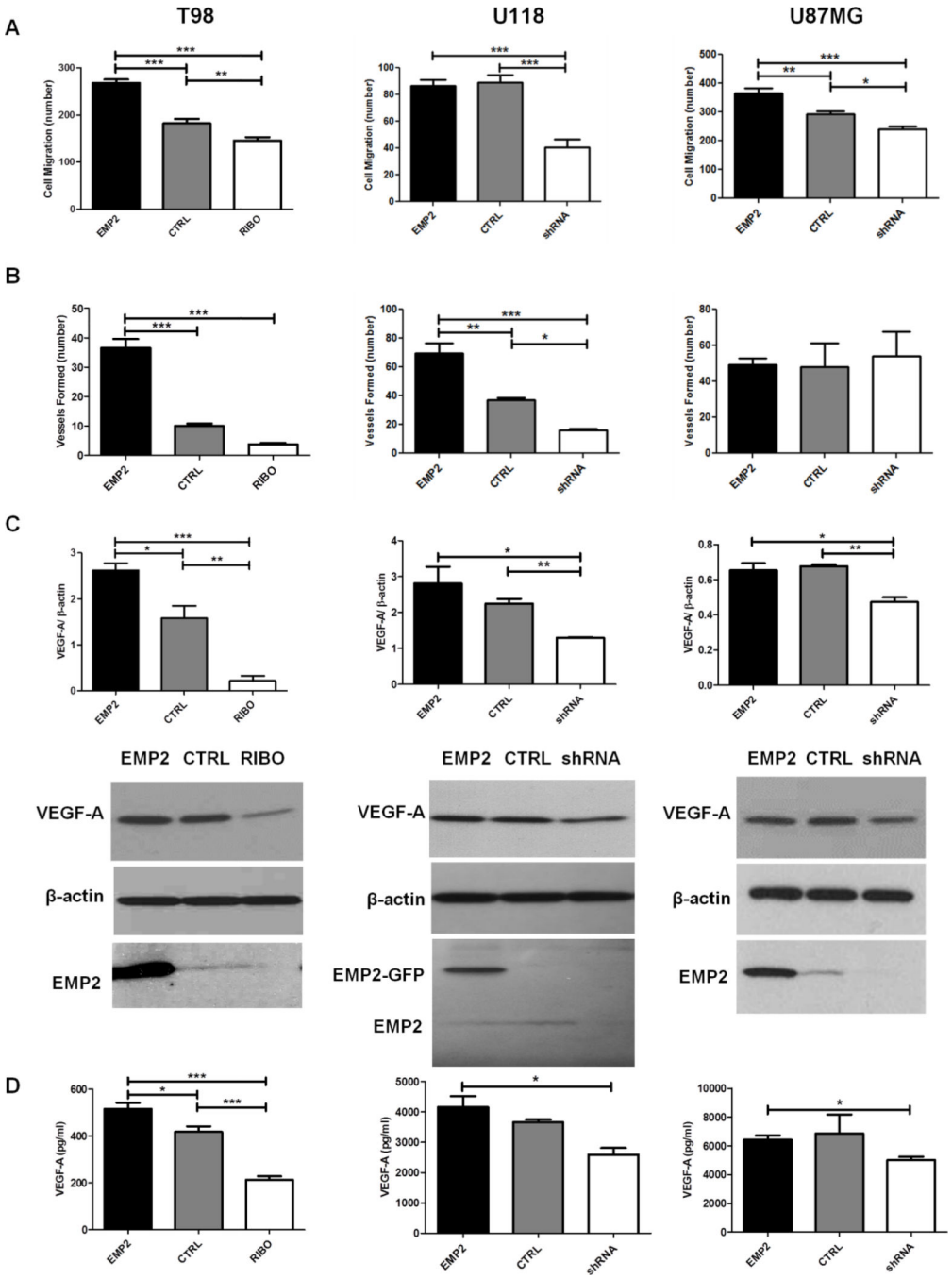

FIG 2. EMP2 Potentiates HUVEC Migration and Tube Formation and Increases VEGF-A Expression and Secretion *in vitro*

T98, U118 or U87MG cells with different levels of EMP2 were cultured for 48 hours and conditioned media were collected at the end of incubation. (A) HUVEC migration assay and (B) capillary tube formation were performed as described in methods. Migratory cell numbers were averaged by counting four random fields per transwell under 400× magnification using a bright field microscope with the averaged results presented. Tube formation was evaluated under a fluorescent microscope and all fully formed tubes were counted on the entire cover slips. The experiment was repeated three times, and the averaged

results presented. (C) T98, U118 or U87MG cells with different levels of EMP2 were cultured for 48 hours and cells were lysed to evaluate VEGF-A expression by Western Blots. Quantification of VEGF-A expression normalized by β-actin were determined by NIH Image J software (top) and representative images of Western Blots show the expression of VEGF-A, EMP2, or β-actin (bottom). (D) T98, U118 or U87MG with different levels of EMP2 were cultured for 48 hours and conditioned media were collected at the end of incubation. Secreted VEGF-A levels in conditioned media were examined by VEGF-A ELISA. The experiments were performed in triplicate or duplicate and repeated at least three times. One-way analysis of variance with a Bonferroni post-test was calculated to determine the difference among three groups. Significance was not reached in U87MG panel by one-way analysis of variance, a student's *t* test was performed between U87MG/EMP2 and U87/shRNA. Significance was defined as $*p<0.05$, $** p<0.001$, $*** p<0.0001$.

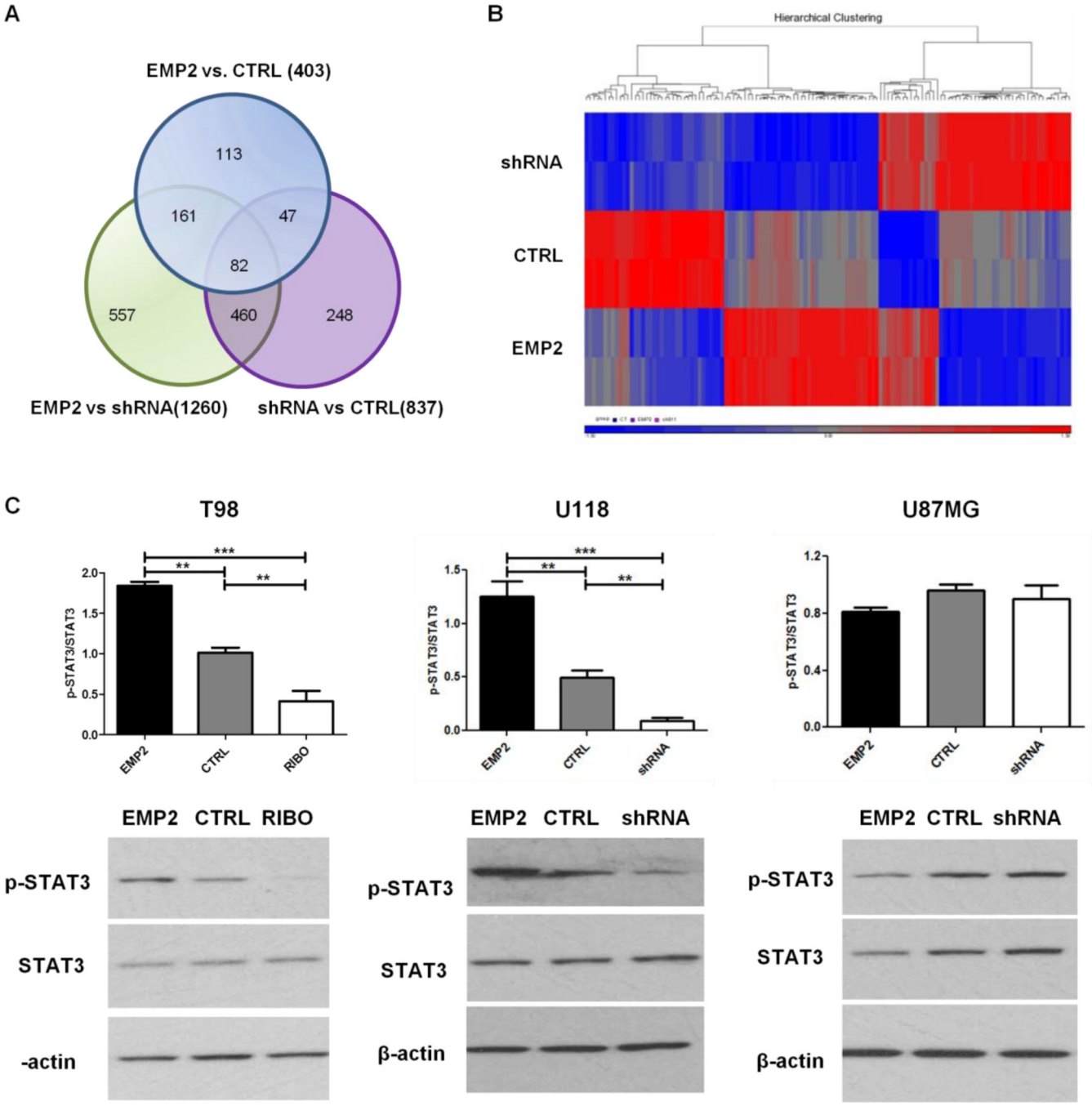

FIG 3. U118 Affymetrix RNA Microarray and EMP2 Regulates STAT3 in Some GBM Cells

RNA was extracted from U118/EMP2, U118/CTRL or U118/shRNA. Affymetrix U133 plus 2.0 microarrays were performed in duplicate and the average of two samples was taken. The relative abundance of specific gene expression was determined among groups. (A) Gene expression was detailed between groups in a Venn diagram. (B) 129 genes were expressed more than 1.5 fold between groups and heat map analysis displayed the differential gene profiling hierarchy among three groups using R software. (C) T98, U118 or U87MG cells with different levels of EMP2 were cultured for 48 hours and cells were lysed to evaluate

total STAT3 expression as well as STAT3 phosphorylation at Y705 by Western Blots. Quantification of STAT3 phosphorylation normalized by total STAT3 expression were determined by NIH Image J software (top) and representative images of Western Blots showed the expression of p-STAT3, STAT3 or β-actin (bottom). The experiments were repeated at least three times. One-way analysis of variance with a Bonferroni post-test was calculated to determine the difference among three groups. Significance was defined as ** $p<0.001$, *** $p<0.0001$.

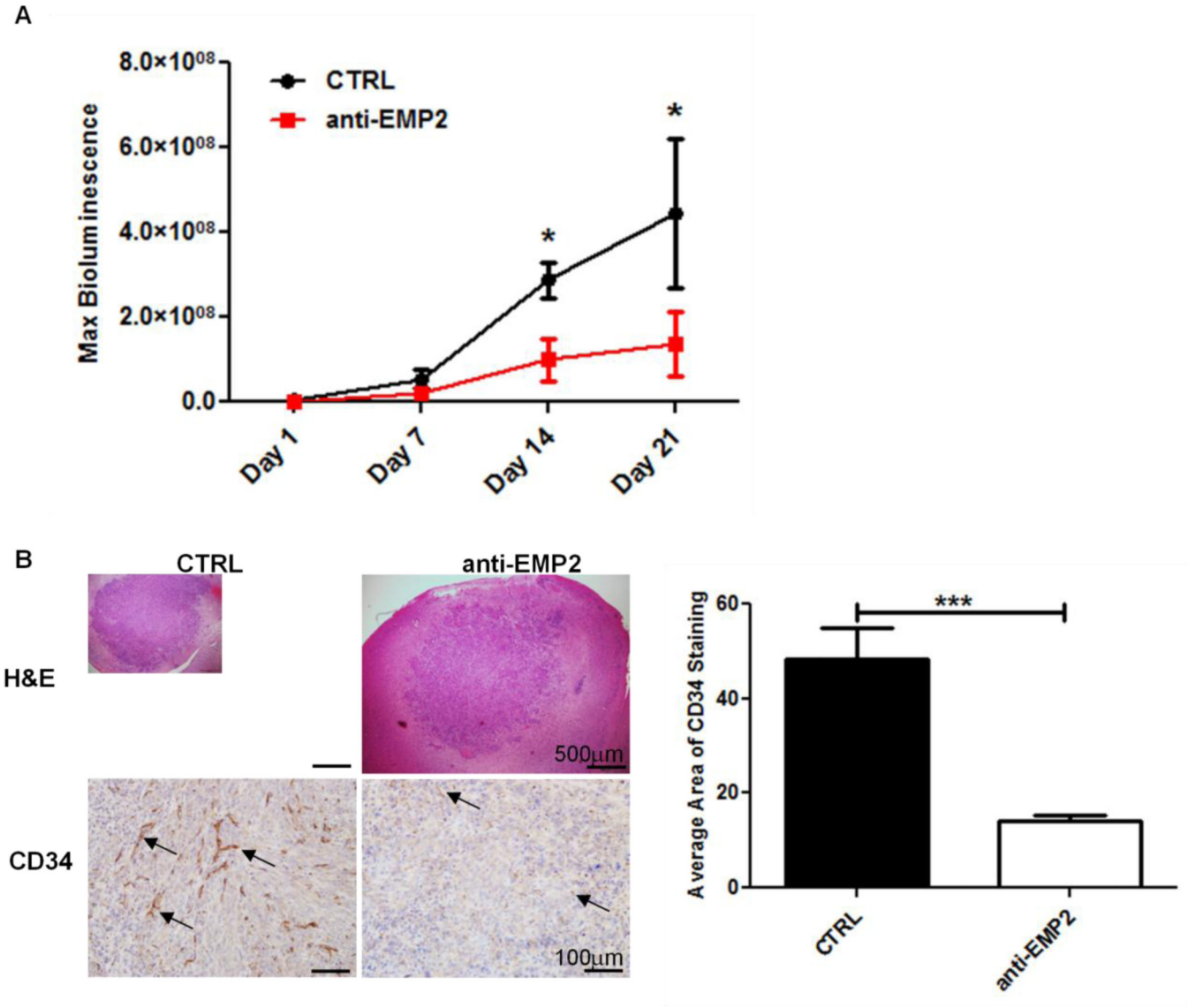

FIG 4. Anti-EMP2 Reduces Intracranial U87MG/EMP2 Tumor Load and Angiogenesis

U87MG/EMP2/Luc cells were stereotactically implanted into athymic nude mice. From day 1, mice were intraperitoneally injected with either control vehicle saline (n=5) or anti-EMP2 IgG1 antibody (n=6) twice a week for three weeks. (A) Bioluminescence images were captured on days 1, 7, 14 and 21 post tumors implantation to monitor tumor growth. A two-way analysis of variance was used to determine the difference between control and anti-EMP2 antibody treatment groups within the treatment time course. (B) Representative histological images (left, top) and CD34 staining (left, bottom) of intracranial tumors from two groups were displayed under 40× and 200× magnification, respectively, and staining was automated quantification using NIH Image J software with a custom macro script were examined (right). Student's *t* test was used to determine the difference between the two groups. Significance defined as *p<0.05, *** p<0.0001.

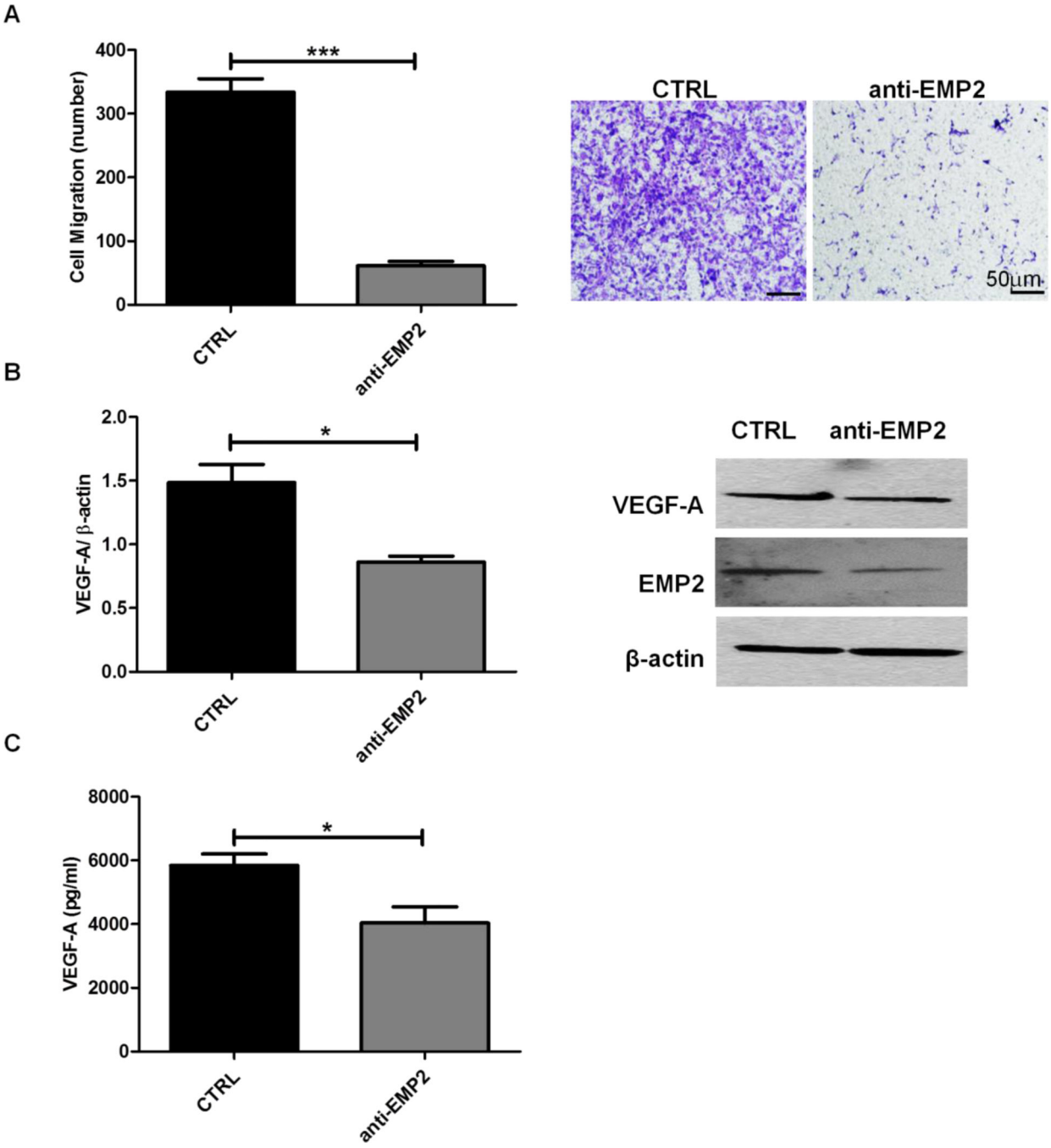

FIG 5. Anti-EMP2 Decreases HUVEC Migration and VEGF-A Expression and Secretion

U87MG wild type cells were cultured in the presence of anti-EMP2 antibody (n=4) or a vehicle (saline) control (n=3) for 48 hours. (A) Conditioned media were collected at the end of incubation for HUVEC migration assay. Migratory cell numbers were averaged by counting four random fields per transwell (left) and representative images of migratory cells were shown under 400× magnification (right). (B) Quantification of VEGF-A expression normalized by β-actin were determined by NIH Image J software (left) and representative images of Western Blots show the expression of VEGF-A, EMP2, or β-actin (right). (C)

Quantification of cell-secreted VEGF-A levels were determined by ELISA. The experiments were repeated at least three times. Student's *t* test was used to determine the difference between the two groups. Significance was defined as $*p<0.05$, $*** p<0.0001$.